11th International Conference on Fracture Mechanics of Concrete and Concrete Structures
FraMCoS-11
J. M. Chandra Kishen, A. Ramaswamy, S. Ray and R. Vidyasagar (Eds)
https://doi.org/10.21012/FC11.092394

APPROACH FOR DETECTION OF FATIGUE PHASES USING THE EXAMPLE OF HIGH-PERFORMANCE CONCRETE

G. GEBUHR[*], S. ANDERS[*], M. PISE[†], D. BRANDS[†] AND J. SCHRÖDER[†]

[*] Institute of Structural Engineering, Faculty of Architecture and Civil Engineering,
University of Wuppertal, Pauluskirchstraße 11, 42285 Wuppertal, Germany
Corresponding Author Email: gebuhr@uni-wuppertal.de

† Institute of Mechanics, Faculty of Engineering, University of Duisburg-Essen,
Universitätsstraße 15, 45141 Essen, Germany

Key words: High Performance Concrete, Fatigue Phases, Detection of Secondary Creep

Abstract: High-performance concretes (HPC) are an emerging material in modern structural design, enabling the development of ever more robust and slender structures. This mode of construction, however, opens up new problems. While gaining compressive strength, HPC loses deformation capacity, ductility and gets more and more prone to fatigue loading. Hence, special attention needs to be paid to ductility and fatigue scenarios. In this case, HPC are just an example. The outlined approach is applicable to any material that shows a three-stage development of damage during fatigue. It is agreed in literature that the gradient of the secondary creep phase is a good indicator to predict failure. However, at present it is only possible to assess the secondary creep phase retrospectively, i.e. after failure. To the author's knowledge, there is no comprehensive indicator or conclusive approach to determine the onset of the second and third phases of a fatigue process during testing without prior knowledge of the point of failure. Such an approach would offer several advantages, e.g.: Firstly, from a material science standpoint, recognition of reaching the third phase of fatigue during testing is beneficial to stop laboratory tests, e.g. for CT measurements. Secondly, for cycle-jump methods to reduce numerical effort in modelling high-cycle fatigue, knowledge of the evolution of deterioration rate allows a reasonable estimation for the length of the cycle jump without losing precision. It could further be very helpful in structural health monitoring when adjusted to a specific structure. This paper outlines an approach to distinguishing between the different stages of fatigue using uniaxial compression fatigue tests on HPC specimens with a compressive strength of about 90 MPa as an example. Both specimens with and without steel fibres are considered. The aim is to have a clear and reproducible separation of the three phases of the classic S-shape degradation curves. It is taken advantage that no major individual events are to be expected during the secondary creep phase, which ensures a sufficiently constant deterioration rate. Accordingly, it is sufficient to detect the beginning and end of this behaviour. It is evident that the moving standard deviation of the stiffness evolution as a damage indicator has a very high significance in detecting both the beginning and the end of the second fatigue phase. Furthermore, it is shown that the approach can be transferred to completely different framework conditions, in this case to flexural fatigue of the mentioned HPC and compressive fatigue tests on normal strength concrete with only slight changes adjustment in parameters.

1 INTRODUCTION AND STATE OF THE ART

For the description of the degradation behaviour of a specimen loaded in fatigue, various damage indicators are considered in literature. These indicators are derived from different concepts and can, for example, be based on measured deformations, see [1–3], energetic or acoustic indicators, see [3–7] or computer tomographic methods, see [8,9]. Most common, are damage indicators that can be calculated from deformation or strain measurements using e.g. strain gauges, LVDTs or laser distance devices.

As damage indicators, most often development of strain or stiffness is plotted against the number of load cycles, see e.g. [6,7,10], as shown in Figure 1. The processes of fatigue of concrete classically takes place in a three-phase progression, often also referred to as S-curve. In the first phase, non-linear accumulation of damage takes place, which is said to manifest in micro-cracking [11]. The cracks remain small and sufficiently dispersed to prevent catastrophic failure, see [10]. Damage development becomes almost linear independent of the damage indicator under consideration. Only in the final failure phase III start to form larger crack clusters and. Depending on the brittleness of the concrete in question, these will lead to the failure of the component at varying speeds. In this phase, the damage process is non-linear again with an increasing gradient of damage per cycle.

The division into these three phases is derived almost exclusively empirically in literature and usually only takes place with knowledge of the entire fatigue process up to failure. Different researchers have described qualitatively, that transition between phases depends on the compressive strength of tested concrete. It is said, that phases I and III get shorter with an increasing compressive strength [12,13]. Absolute and relative changes in different damage indicators are also of limited use as they depend on the compressive strength of the concrete being investigated. Increasing brittleness of concrete with high compressive strengths can also be seen in fatigue.

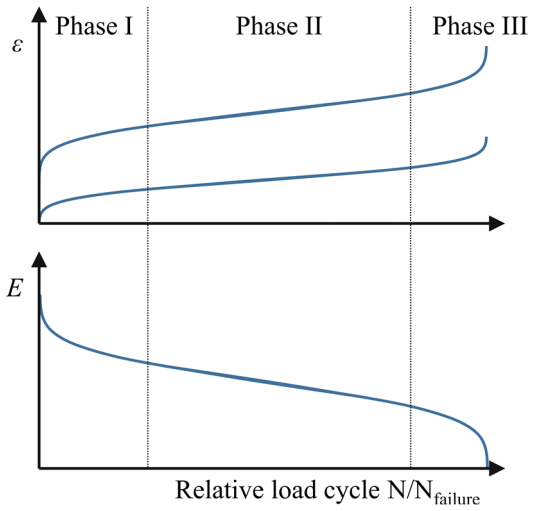

Figure 1: Qualitative phases of fatigue.

Table 1: Relationship between compressive strength and stiffness development until failure.

Compressive strength	Stiffness loss up to Phase III	Source
40 N/mm²	~40 %	[6]
70 N/mm²	~30 %	[7]
90 N/mm²	~15 - 25 %	[14]
110 N/mm²	~5 - 15 %	[14]

In Table 1 the total reduction in stiffness throughout different fatigue tests is summarised. It is evident that the stiffness reduction generally decreases with increasing compressive strength.

This means that the gradient of the second phase cannot be used for the phase classification directly, as it depends on compressive strength of the concrete. Secondly, the identification is more difficult for high strength concrete because changes in gradient are smaller.

An approach to phase classification is also given in [15], but this again requires knowledge of the load cycle count to failure.

There is also a correlation between the strain development and the number of load cycles to failure. In [16,17], for example, an approach is outlined to model this with a linear-logarithmic regression. There, the formula

$$\log N = C_1 - C_2 * \log \varepsilon_{II} \tag{1}$$

gives a relationship between the logarithmised number of cycles to failure N and strain

development with C_1 and C_2 as test-specific coefficients over which the regression is applied. Again, the number of load cycles until failure is required for a statement.

An additional factor complicating the identification of phases is that fatigue damage inherently is subject to distinct scattering, see [18].

An approach to determine phase transitions should therefore require the least possible knowledge about the total duration of the experiments. In summary, a generalised phase classification applicable in running tests is desirable for various reasons, but not generally implemented.

2 EXPERIMENTS STUDIED FOR CALIBRATION AND EVALUATION

The approach presented here is established in several steps: Firstly, the basic idea and calibration on test series A is presented. Here, uniaxial compression fatigue tests on cylinders with a height of 300 mm and a diameter of 150 mm made of high performance concrete (HPC) were used. The specimen had a 28-day compressive strength of 102 N/mm² under static loading. In total, two specimens are chosen in this context, one without fibres and one with 57 kg/m³ of steel fibres with hook ends. The fibres have a diameter of 0.92 mm, a total length of 60 mm and a tensile strength of 1160 N/mm². Fatigue loading was applied at a loading frequency of 1 Hz with a lower level of 5 % and an upper load level of 75 % of the compressive strength were applied. Deformation was measured with three longitudinally applied LVDTs.

Then, the transferability of the approach to two other framework conditions is demonstrated. Here, on the one hand, another uniaxial compression fatigue test from test series B with a different specimen geometry and compressive strength as well as a reduced upper load level, is used. The dimensions here are 180 mm in height and 60 mm in diameter, the compressive strength class was C25/30, which is in the normal strength concrete (NSC). In series B load was applied at a frequency of 0.1 Hz. Again, the deformation was measured using LVDTs along the sides of the specimen.

Finally, a flexural fatigue test on a beam made of the aforementioned HPC mixture with 57 kg/m³ fibres taken from test series C is looked into. This experiment was conducted on a notched beam with dimensions of 150 x 150 x 700 mm³ tested in flexure. In this test, the lower and upper load levels were 5 % and 75 % of the limit of proportionality, respectively. Here, the load was applied at a frequency of 1 Hz.

The data acquisition-rate was 100 times the loading frequency for all tests considered.

Both concrete compositions are listed in Table 2.

Table 2: Concrete mixtures.

Ingredient	NSC kg/m³	HPC kg/m³
CEM I 42.5 R	290	-
CEM I 52.5 R	-	500
Quartz powder	40	-
Aggregate 0/2	791 Quartz	925 Quartz
Aggregate 2/8	966 Quartz	920 Basalt
Superplasticizer	0.9	5
Stabilizer	0.3	3
Water	203	176
Steel fibres	-	0 / 57

3 APPROACH

The approach is based on the relative stiffness as a damage indicator s_i, i.e. the gradient modulus of any given hysteresis loop s_p relative to the initial stiffness s_0 as shown in Figure 2. In principle, the outlined approach can also be applied to other damage indicators.

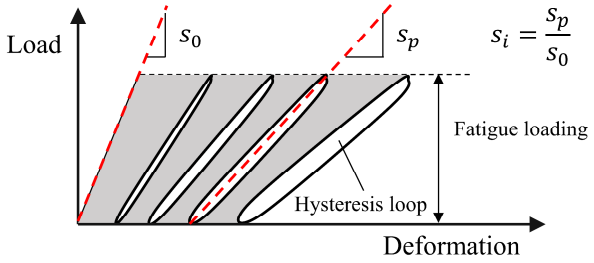

Figure 2: Definition of the relative stiffness s_i as exemplarily chosen damage indicator.

As stated, fatigue formulated by a deformation-based indicator such as the stiffness, is defined by an S-curve with three phases as illustrated in Figure 3 a).

While phase I and phase III of the curve are nonlinear, phase II is approximately linear. In order to subdivide the fatigue process, it is intended to identify the beginning of the second phase of the linear damage development. For this purpose, e.g. derivates of the development of the initial indicator with respect to the number of load cycles could be used. As illustrated in Figure 3 b), a derivate should show a plateau in the area of the second fatigue phase. Potentially, higher derivates could be considered. However, depending on the approach chosen, this may not be necessary or may even dilute the results.

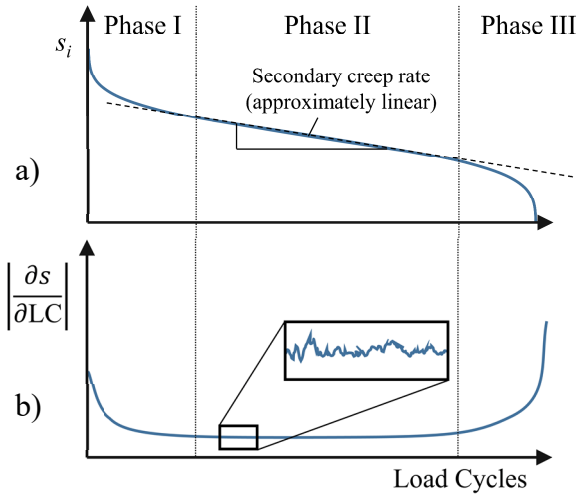

Figure 3: Usual classification of fatigue phases, a) scheme for stiffness as damage indicator and b) according derivate with regard to load cycles.

Upon closer examination it is noticeable that all data is subject to various influencing factors that provide for significant variations in the linearity of the second fatigue phase. Some can be traced back to cracking events, especially in flexural tests of steel-fibre reinforced concrete. Hence, these events are of relevance for the damage evaluation, while others are undesirable interfering factors from other sources. The latter include, for example, statistical factors like inherent noise in the measurement of the recording instruments or daily changes in temperature in the lab.

This combination of noise and the relatively small sought-after changes in the damage indicators themselves per load cycle becomes problematic when looking directly at derivate. The higher the degree of derivate, the more specific characteristics of the individual fatigue phases may get lost. In order to obtain a clearly separable second phase nevertheless, various statistical methods can be applied. In the given context, the following statistical characteristics are used:

1. Simple moving mean – for each relative stiffness of a load-cycle s_i, the simple moving mean $SMA_k(s_i)$ is the unweighted average over a k-value window of data points preceeding s_i, including s_i itself. It is defined as:

$$SMA_k(s_i) = \frac{1}{k}\sum_{n=i-k+1}^{i} s_n \qquad (2)$$

2. Moving standard deviation – the standard deviation $MSTD_k(s_i)$ of the data set with respect to the moving mean $SMA_k(s_i)$ mentioned above, defined as:

$$MSTD_k(s_i) = \sqrt{\frac{1}{k}\sum_{n=i-k+1}^{i} \left(s_n - SMA_k(s_i)\right)^2} \qquad (3)$$

Accordingly, the evaluation of data using the moving standard deviation acts like a derivate itself due to the reference to the moving average value. Only the reference to the change in stiffness ∂s on individual load cycles ∂LC is replaced by k load cycles. To highlight the significance, Figure 4 shows a comparison of the derivate with respect to ∂LC to the $MSTD_k(s_i)$ using the example of a specimen from test series A with 57 kg/m³ fibres. The window size k was set to 1 % of the number of load cycles until failure as this turned out a good reference value. Here, the entire test was known. However, comparison with other datasets shows that a rough estimate of the number of cycles was sufficient. While calculation of the moving standard deviation does not remove all statistical noise, a plateau can still be seen spanning the entire phase II of fatigue. Sufficient accuracy can already be achieved in this example if a static limit in the standard deviation is chosen.

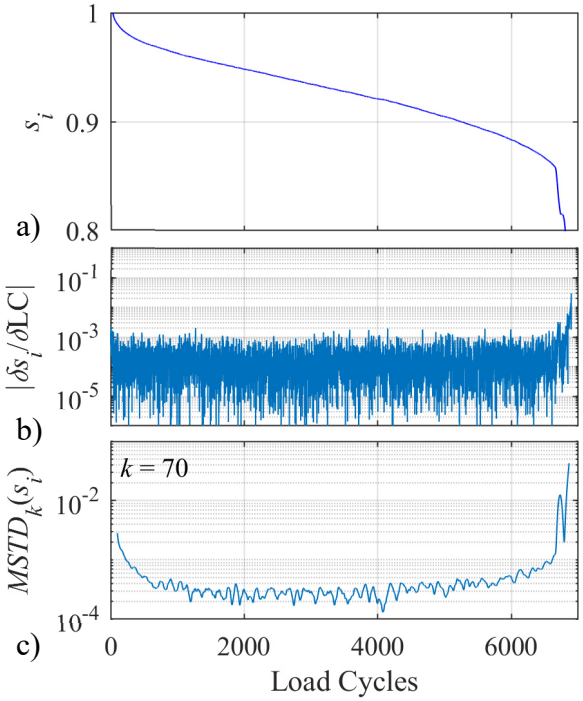

Figure 4: Uniaxial compression fatigue of an HPC specimen with fibres, test series A. a) Development of relative stiffness, b) corresponding derivate with respect to ∂LC and c) moving standard deviation $MSTD_k(s_i)$.

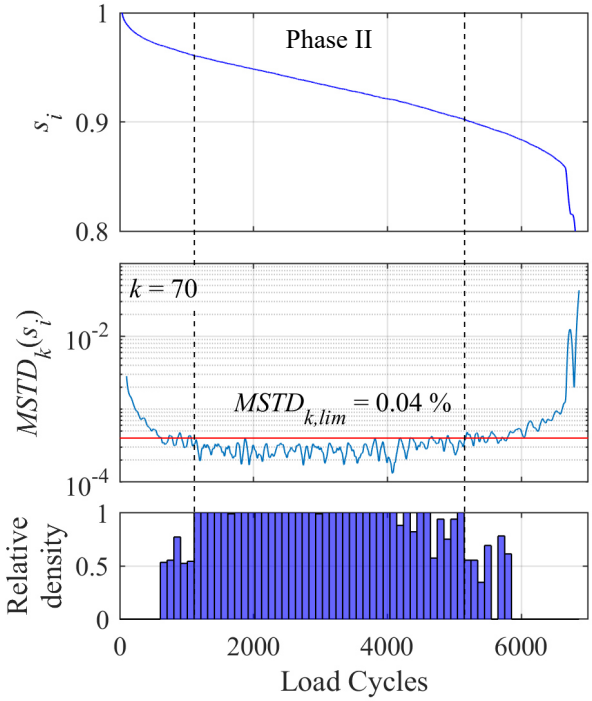

Figure 5: Combined approach for phase definition, extended from Figure 4. 7000 load cycles to failure.

To further minimize the influence of the remaining noise, a second optimization step is performed. First, a rough estimation of the plateau of the standard deviation is carried out. In the given data set, a value as low as $MSTD_{k,lim} = 0.04\,\%$ is suitable. Now, the relative density of standard deviations below this threshold is used. This is achieved by dividing the data set into ranges of size k. Then, for each range, the ratio of the moving standard deviations below the threshold value $MSTD_{k,lim}$ to the total number of values contained in the last k values is formed. This is illustrated in Figure 5 as histogram.

Note, that $MSTD_k(s_i)$ is only calculated after a full k-sized window is available to avoid boundary effects. I.e. in this case the first considered value is evaluated starting at the 70^{th} load cycle.

This makes it possible to define phase II as a range characterised by the first and last occurrence of a relative density of the sought standard deviations being 1.0.

Thus, despite the relatively large number of steps taken to identify the second fatigue phase, the procedure generally requires only two control variables. The window size k and a threshold value for the density of standard deviations $MSTD_{k,lim}$. As supplementary tests have shown, both allow reliable identification of the fatigue phases already by rough estimation.

Figure 6 shows another cylinder from test series A, in this case a fibre-free specimen with a small number of cycles to failure. This example considers the influence of a changed window size k relative to the total number of cycles. Here, k was set to the same value as in the previously considered data set. Due to the overall lower number of load cycles until fatigue failure of the specimen, this corresponds to 5 % of the load cycles until fatigue. Nevertheless, the plateau of the standard deviation remains, again the phases can be clearly identified. Again, the first k values are not calculated, until 70 cycles have passed.

However, it has been shown that the two parameters necessary for the approach can be estimated with sufficient accuracy even during an ongoing experiment.

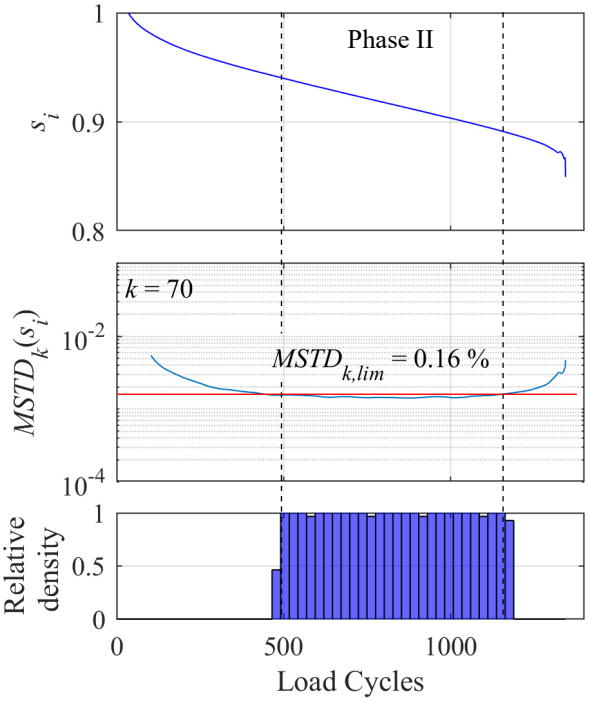

Figure 6: Uniaxial compression fatigue of HPC without fibres from test series A. 1350 load cycles to failure.

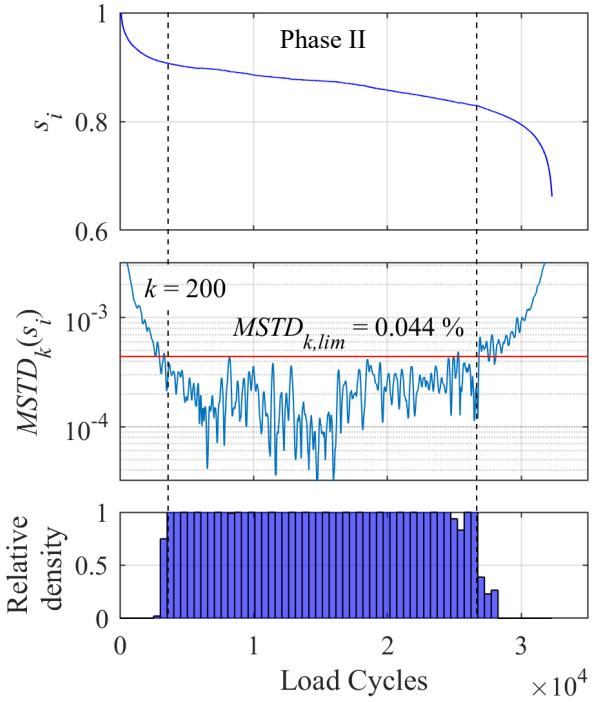

Figure 7: Uniaxial compression fatigue of NSC from test series B. 32300 load cycles to failure.

Furthermore, as the algorithm only uses values from past load cycles, a change in fatigue phase can also be detected during an ongoing experiment.

It was found, that there are threshold values for k. For all specimens considered in the wider scope of the study, this was around $k = 10$ load cycles on the lower end for a useful prediction. A maximum value for k as such was found to be primarily based on the expected amount of load cycles until fatigue. Larger window sizes generally provide smoother curves while smaller window sizes allow an earlier detection of phase changes. It can also be noted that similar experimental frameworks also achieved similar magnitudes for the limit values $MSTD_{k,lim}$ required for phase identification when k was kept unchanged.

4 TRANSFERABILITY

4.1 Choice of examples

In the following, the transferability of the presented approach to other framework conditions is shown. In a first example, another specimen in uniaxial compression is considered.

This aims to demonstrate the applicability to lower strength concrete, see Section 4.2. To illustrate that the approach is also independent of the type of loading, its transfer to flexural stress fatigue is then shown in Section 4.3.

4.2 Normal strength concrete in compressive fatigue

Figure 7 shows a preparation of a data set from a specimen from test series B. The specimen, part of a fatigue creep study from [19], has an h/d ratio of 3:1 as described with smaller overall dimensions. It was loaded at a frequency of 0.1 Hz to 65 % of the static failure load. The changed framework conditions of the test setup do not seem to show any major influence on the general applicability of the approach here. Despite a window size k of only about 0.7 % of the cycles to failure, a distinct second fatigue phase is again obtained, thus proving the applicability of the method.

4.3 HPC in flexural testing

Figure 8 shows a study of a flexural beam from test series C, a fibre modified HPC. In this context, the introduction of fibres also results in two successive fatigue processes, see [1–3].

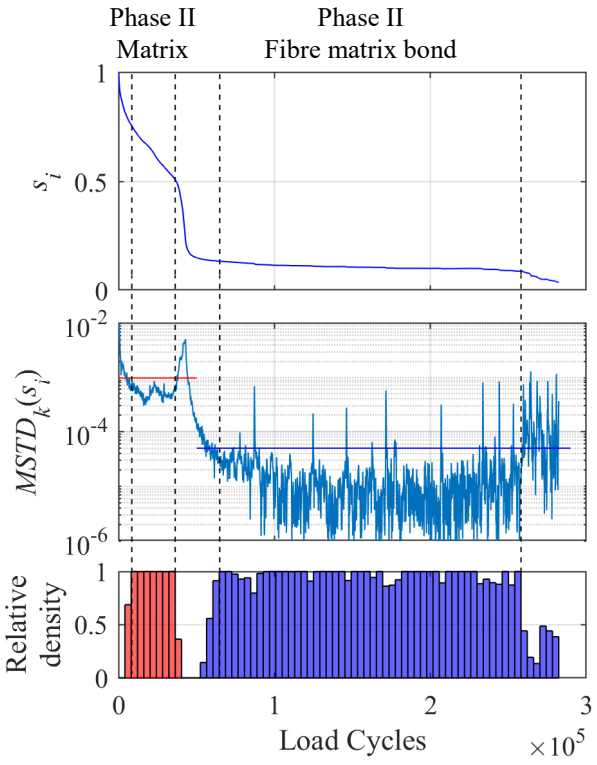

Figure 8: Flexural fatigue of HPC form series C with distinct matrix and fibre-matrix fatigue, 282.400 load cycles to failure, $k = 200$, $MSTD_{k,lim,concrete} = 0.1$ % (red) and $MSTD_{k,lim,fiber} = 0.005$ % (blue).

First, the concrete matrix degrades before a crack is initiated, the fibre load-bearing effect is not yet significantly activated. Then, a crack opens and the fibre-matrix bond degrades in fatigue. For both processes, degradation of matrix and successive degradation of fibre load bearing mechanism, a separate plateau in the standard deviation results successively. The transition between the two processes, however, results in a pronounced peak in standard deviation which allows for a clear differentiation between the two fatigue processes. In further experiments it has been found that the limit values necessary to identify these plateaus are dependent on the amount of fibres.

Despite the fact that the total number of load cycles to failure of the specimen is about ten times higher than in the tests shown before, the window size k was again set to 200. Higher values would smooth the fatigue process of the fibre-matrix bond more strongly.

The comparatively low value for k was primarily chosen to illustrate again that only a rough estimate is needed for the window size.

The fatigue process of the fibre-matrix bond also shows clear fluctuations in the standard deviation, which appear to be almost cyclic in nature. This can be attributed to the fact that a large number of fatigue processes of individual fibre-matrix bonds take place due to the large number of fibres introduced. However, it can be seen that the material can redistribute the loss of stiffness from these fibres to other fibres in the cross-section.

Overall it can be seen that the approach presented does allow a phase classification for fatigue, even when applied to completely different experimental framework conditions and decoupled from the number of load cycles.

5 SUMMARY AND OUTLOOK

5.1 Summary

In this paper, a generalised approach for identifying individual fatigue phases is outlined and applied on different concrete materials in different framework conditions. This includes data sets for high-performance concrete in uniaxial compression fatigue and flexural fatigue tests with and without fibres as well as uniaxial compression fatigue on normal strength concrete with dimensions and a lower loading frequency. Overall, it was found that when considering the standard deviation in development of the relative residual stiffness as a damage indicator, two values are sufficient to identify a transition between the three phases of the typically S-shaped curve of the fatigue progression. These are:

1. a window of size k load cycles over which a moving standard deviation of the relative stiffness is calculated, and
2. a limit value $MSTD_{k,lim}$ for the moving standard deviation, below which the standard deviation is regarded as constant in the second phase of fatigue.

Both values can be estimated in preliminary tests as well as during a running test. It is also important that the moving window always refers to the k values preceding the current load

cycle. This ensures that an evaluation of the current fatigue phase is possible at any time during a running test. For size k at least 10 load cycles should be taken into account in order to guarantee meaningful results. Such a limit for a maximum window is actually only given by the (expected) total number of cycles until fatigue of a specimen. However, it has turned out, that a maximum of about 2000 values for the window size is reasonable.

For the threshold value $MSTD_{k,lim}$, it was shown that, despite the direct coupling to the window size k, similar magnitudes can also be assumed as expected values under comparable experimental conditions.

For all examples presented in this study, the relative residual stiffness was taken as damage indicator. Nevertheless, other well-known indicators such as development of strain can be applied in this approach more or less equally good.

Overall, the discriminatory power of the approach seems to be capable of enabling the identification of phase transitions in fatigue. It thus represents a tool for studying the fatigue process of brittle materials as a whole.

5.2 Outlook

The outlined approach provides a comprehensive and adaptable tool to detect the beginning and end of the second phase of fatigue with good reproducibility. However, in the form presented here, simplifications are made in some places. E.g. for the window size k, while showing good selectivity already, more comprehensive studies for a better estimation of the values to be applied are in process. Meanwhile, the static limit value $MSTD_{k,lim}$ is currently chosen mainly for its simplicity. For example, a more detailed analysis of the underlying trends of the moving standard deviation curve can possibly provide a more differentiated result. If this static border criterion will be kept, the definition of the second phase by relative density can be adjusted. Currently, the second fatigue phase is defined by the range between the first and last k-sized window in which *all* standard deviations lie below the limit value $MSTD_{k,lim}$. This static consideration is potentially subject to smaller fluctuations and will therefore be optimised. No additional limit value or further optimisation step was inserted in this paper. An additional limit value for the relative density lower than 1.0, would obvious be beneficial in order to compensate for smaller fluctuations. In addition, more sophisticated density distribution functions could be utilised, such as outlaid in [20].

As it is the aim to provide an approach that is able to detect the beginning of the second and third phase during a running tests, an algorithm will be developed to adapt the values k, $MSTD_{k,lim}$.as well as the threshold value for the density in the course of testing. Furthermore boundary values as ratios e.g. between the window size k and threshold for the density are currently being developed.

Finally, a more detailed consideration of other influences such as temperature is also still pending at this point, even if, as described, the influence is already minimised by the approach in the first considerations.

6 ACKNOWLEDGEMENTS

This research has been funded by the Deutsche Forschungsgemeinschaft (DFG, German Research Foundation), project number 353513049 (AN1113/2-2, BR5278/2-2, SCHR570/32-2) within the DFG Priority Programme 2020 “Cyclic deterioration of high performance concrete in an experimental-virtual lab”.

7 REFERENCES

[1] Gebuhr G., Anders S., Pise M., Brands D. and Schröder J., 2022. Damage development of steel fibre reinforced high performance concrete in high cycle fatigue tests. In: *Current Perspectives and New Directions in Mechanics, Modelling and Design of Structural Systems*; Zingoni, Alphose(ed). London: CRC Press; pp. 1327–1332.

[2] Gebuhr G., Anders S., Pise M., Sahril M., Brands D. and Schröder J., 2019. Deterioration development of steel fibre reinforced high performance concrete in

low-cycle fatigue. In: *Advances in Engineering Materials, Structures and Systems: Innovations, Mechanics and Applications*; Zingoni, Alphose(ed). CRC Press; pp. 1444–1449.

[3] Gebuhr G., Pise M., Anders S., Brands D. and Schröder J., 2022. Damage Evolution of Steel Fibre-Reinforced High-Performance Concrete in Low-Cycle Flexural Fatigue: Numerical Modeling and Experimental Validation. *Materials (Basel)*; **15**.

[4] Smedt M. de, Vandecruys E., Vrijdaghs R., Verstrynge E. and Vandewalle L., 2022. Acoustic emission-based damage analysis of steel fibre reinforced concrete in progressive cyclic uniaxial tension tests. *Construction and Building Materials*; **321**:126254.

[5] Scheiden T., Oneschkow N., Löhnert S. and Patel R., 2019. Acoustic emission due to fatigue damage mechanisms in high-strength concrete with different aggregates. In: *Advances in Engineering Materials, Structures and Systems: Innovations, Mechanics and Applications*; Zingoni, Alphose(ed). CRC Press; pp. 1491–1496.

[6] Holmen J.O, 1979. Fatigue of Concrete by Constant and Variable Amplitude Loading. Division on Concrete Structures, Norwegian Institute of Technology, University of Trondheim.

[7] Petković G., Rosseland S., Stemland H., 1992. Fatigue of high strength concrete, A-92128. Trondheim: SINTEF.

[8] González D.C., Mena A., Mínguez J. and Vicente M.A., 2021. Correlation between the fiber content and orientation and the mechanical behaviour of fiber-reinforced concrete subjected to static and cyclic three point bending test by the use of CT-Scan technology. In: *Bridge Maintenance, Safety, Management, Life-Cycle Sustainability and Innovations;* Yokota, Hiroshi, et al.(eds). CRC Press; pp. 2697–2704.

[9] Oneschkow N., Scheiden T., Hüpgen M., Rozanski C. and Haist M., 2021. Fatigue-Induced Damage in High-Strength Concrete Microstructure. *Materials (Basel)*; **14**.

[10] Thiele M., 2016. Experimentelle Untersuchung und Analyse der Schädigungsevolution in Beton unter hochzyklischen Ermüdungsbean-spruchungen [Ph.D Thesis]: Bundesanstalt für Materialforschung und-prüfung (BAM).

[11] Park Y.J., 1990. Fatigue of Concrete under Random Loadings. *J. Struct. Eng;* **116**:3228–35.

[12] Oneschkow N 2014. Analyse des Ermüdungsverhaltens von Beton anhand der Dehnungsentwicklung [Ph.D Thesis]: Gottfried Wilhelm Leibniz Universität Hannover.

[13] Lohaus L, Anders S, Wefer M., 2007. High-cycle fatigue of ultra-high performance concrete (uhpc) - fatigue strength and damage development. In: *3rd Int. Conference on Lifetime Oriented Design Concepts, proceedings*; pp. 257–265.

[14] Do M.-T., Chaallal O. and Aïtcin P.-C., 1993. Fatigue Behavior of High-Performance Concrete. *J. Mater. Civ. Eng;* **5**:96–111.

[15] Pfanner D., 2003. Zur Degradation von Stahlbetonbauteilen unter Ermüdungs-beanspruchung. [Ph.D Thesis]: Bochum, Ruhr-Universität, 189. Düsseldorf: VDI-Verl.

[16] Cornelissen H. and Reinhardt H.W., 1984. Uniaxial tensile fatigue failure of concrete under constant-amplitude and programme loading. *Magazine of Concrete Research*; **36**:216–26.

[17] Weigler H. and Rings K.H., 1985. Unbewehrter und bewehrter Beton unter Wechselbelastung, Plain and reinforced concrete under cyclic loading, Betonwerk Fertigteil-Tech. *Betonwerk Fertigteil-Tech*; **51**:705–13.

[18] Ortega J., 2019. Error in the probabilistic characterisation of concrete fatigue. In: Conference on Fracture Mechanics of Concrete and Concrete Structures. In: *10th International Conference on Fracture Mechanics of Concrete and Concrete*

Structures, proceedings; Pijaudier-Cabot, G. et al.(ed). 23-26 June 2019.

[19] Weber F.M. and Anders S., 2023. Fatigue Damage versus Creep Deformation – Differentiation using the Development of Stiffness. In: *11th International Conference on Fracture Mechanics of Concrete and Concrete Structures, proceedings*; Kishen, J. M. et al(ed); in press.

[20] Cao R., Cuevas A. and González Manteiga W., 1994. A comparative study of several smoothing methods in density estimation. *Computational Statistics & Data Analysis*; **17**:153–76.